American Mineralogist, Volume 91, pages 211–215, 2006

Complete solid-solution between $Na_3Al_2(PO_4)_3$ and $Mg_3Al_2(SiO_4)_3$ garnets at high pressure

FABRICE BRUNET,[1,*] VINCENT BONNEAU,[1] AND TETSUO IRIFUNE[2]

[1]Laboratoire de Géologie, CNRS-UMR8538, Ecole Normale Supérieure, Paris, France
[2]Geodynamics Research Center, Ehime University, Matsuyama 790-8577, Japan

ABSTRACT

Syntheses along the $Mg_3Al_2(SiO_4)_3$-$Na_3Al_2(PO_4)_3$ join were carried out in the 15–17 GPa range at temperatures between 1200 and 1600 °C. An $Na_3Al_2(PO_4)_3$ compound of garnet-like structure, with a cubic-cell parameter of 11.579(2) Å, was synthesized and characterized. Intermediate compositions are also found to crystallize in the garnet structure. Between pyrope and $Na_3Al_2(PO_4)_3$, the cubic unit-cell volume increases by 3.1%. In addition, nominal compositions, $Mg_{2.5}Na_{0.5}Al_2Si_{2.5}P_{0.5}O_{12}$ and $Mg_2Na_1Al_2Si_2P_1O_{12}$, were run at 3 GPa and 875 °C. They yielded garnet, among other phases, but with no significant phosphorus incorporation as indicated by a pyrope-like unit-cell volume. Phosphorus content in pyrope from the UHP Dora-Maira quartzites appears as a potential pressure indicator where UHP garnet coexists with phosphate minerals. The P-content in upper mantle garnets can be used as a probe of phosphorus activity in the host rock.

Keywords: Crystal synthesis, phosphate garnet, high-pressure studies, garnet, petrography, phosphorus in garnet, XRD data, P-Si garnet solid-solution series

INTRODUCTION

The garnet structure can accommodate, in its eightfold coordinated site, minor amounts of cations with a large ionic radius as Na or Y (Meagher 1980). Sodium contents up to 0.25 wt% Na_2O have been analyzed in upper-mantle garnets (Sobolev and Lavrent'ev 1971; Reid et al. 1976; Bishop et al. 1978). Extremely high sodium-concentrations of up to 1.03 wt% have been reported from garnet inclusions in diamonds from the Monastery Mine kimberlite pipe (Moore and Gurney 1985). High Na-contents in garnet from upper-mantle eclogite have been used to infer the likely occurrence of diamond (McCandless and Gurney 1989; Schulze 1992), since the highest Na contents are usually encountered in garnets from diamond-bearing eclogites (Sobolev and Lavrent'ev 1971). Like potassium in clinopyroxenes (Sobolev and Shatsky 1990), high Na-contents in garnet could be related to high pressure. In fact, Smith and Mason (1970) analyzed a sodium-bearing majorite garnet containing 0.5 wt% Na_2O in the shocked Coorara chondrite. This apparent sodium affinity for the garnet structure at high-pressure has been confirmed experimentally. Pioneer experimental work by Ringwood and Major (1971) partly motivated by the, then recent, discovery of Smith and Mason (1970), showed that the Coorara Na-bearing majorite garnet could be synthesized at 25 GPa and 1000 °C. In the Ca-garnet system, a $NaCa_2(AlSi)Si_3O_{12}$ composition was synthesized at 18 GPa, 1000 °C (Ringwood and Major 1971). It appeared therefore that the $^{[VIII]}Na^{[VI]}Si = {}^{[VIII]}Ca^{[VI]}Al$ coupled substitution that involves sixfold coordinated silicon was a possible way to incorporate Na in the garnet structure at very high-pressure. At lower pressure (5 GPa), Ringwood and Major (1971) were able to grow another Na-rich garnet, $CaNa_2Ti_2Si_3O_{12}$, where the Na incorporation is charge-balanced by Ti^{4+} in the aluminum site. The latter substitution appears the most likely to account for the Na content in most upper-mantle garnets recovered at the Earth's surface. Sobolev and Lavrent'ev (1971) claimed, however, that Na_2O contents of up to 0.22 wt% analyzed in garnet from diamond-bearing eclogites are correlated to sixfold-coordinated silicon. Bishop et al. (1978) carried out a similar systematic study. They concluded that Na in garnet could be accounted for by the $NaTiMe^{2+}_{-1}Al_{-1}$ (and $NaPMe^{2+}_{-1}Si_{-1}$) substitution without the need to invoke sixfold coordinated silicon.

Thompson (1975) synthesized from natural tholeitic basalts, in the 1.8–4.5 GPa range for temperatures between 1200 and 1410 °C, garnets containing up to 0.4 wt% Na_2O (and 0.6 wt% P_2O_5). Electron microprobe analyses yielded a clear Na-P correlation indicating that all P incorporated by the garnet structure is accounted for by the $NaPMe^{2+}_{-1}Si_{-1}$ substitution. More recently, Ye et al. (2000) reported high concentrations of P_2O_5 (0.06–0.17 wt%) and Na_2O (0.05–0.06 wt%) in garnets from Yangkou eclogites (Sulu UHP belt, China). Shertl et al. (1991) analyzed 0.06 and 0.09 wt% Na_2O in two pyrope crystals from the coesite-bearing quartzite at the Parigi locality (Dora-Maira, western Alps). Compagnoni and Hirajima (2001) collected a sodium X-ray map on superzoned garnets in other quartzites from the same UHP massif (Brossasco-Isasca unit). Based on the intensity scale of their X-ray map (Fig. 5f in Compagnoni and Hirajima 2001), Na_2O contents of up to 0.09 wt% can be inferred in the pyrope-rich zone. Brunet and Lecocq (1999) showed that these relatively high Na_2O-contents can be accounted for by a $NaPMe^{2+}_{-1}Si_{-1}$ substitution in these garnets where P_2O_5 contents of up to a quarter of a weight percent can be encountered. This coupled substitution and its positive dependence with pressure is supported by the likely stability of a $Na_3Al_2(PO_4)_3$ garnet modification at high-pressure (above 8 GPa, Brunet et al. 2003).

In light of these natural and laboratory data and in relation to the potential of silicate minerals to host phosphorus in the deep Earth (Brunet and Chazot 2001), we have investigated, experimentally, the ability of the garnet structure to incor-

* E-mail: brunet@geologie.ens.fr

porate phosphorus (and sodium) according the $NaPMg_{-1}Si_{-1}$ substitution. A series of compositions were prepared along the $Mg_3Al_2(SiO_4)_3$–$Na_3Al_2(PO_4)_3$ join and run between 15 and 17 GPa in the 1500–1700° C range and, at 3 GPa, 875 °C, in a multi-anvil apparatus and a piston-cylinder press, respectively.

Experimental methods

Starting materials in the MgO-Na_2O-Al_2O_3-SiO_2-P_2O_5 system (Table 1) were obtained either from stoichiometric mixtures of reagent grade oxides or from TEOS-based gels (see Brunet and Chazot 2001). The dry starting material is encapsulated in a platinum tube squeezed at the two ends and hammered in a 1.5 mm diameter die. In addition, two platinum end-disks (50 μm thick and having the capsule inner diameter) are located at each capsule end to improve chemical insulation of the sample powder.

A series of syntheses above 10 GPa were performed in a split-sphere multi-anvil (2000 tons, GRC Matsuyama) using WC anvils of 5 mm truncation edge-length. Two additional experiments at 3 GPa were run in an end-loaded piston-cylinder (ENS, Paris) with gold capsules with 2 mm outer diameter (see Brunet et al. 2003 for more details). The multi-anvil assembly is composed of a semi-sintered (Mg,Co)O octahedron filled with a straight-wall $LaCrO_3$ heater itself sandwiched between two ZrO_2 end-disks that are drilled to fit a molybdenum rod (electrical conductor). The junction of a $W_{97}Re_3/W_{75}Re_{25}$ thermocouple (0.125 mm diameter) is sandwiched between two axial capsules placed in an MgO sleeve in the middle of the $LaCrO_3$ heater.

After the experiments, most of the sample is ground in ethanol for powder X-ray diffraction, the rest is embedded in epoxy plugs and polished for further SEM and electron microprobe characterization. A few mg of ground sample powder are spread on a single-crystal quartz slide for X-ray powder diffraction (XRPD). XRPD data were collected with a MAC Science diffractometer (M21X) equipped with a graphite monochromator and a copper rotating anode (Cu$K\alpha$) operated at 40 kV and 100 mA. Lattice parameters and "zero shift" were retrieved using the non-linear least-squares UnitCell program (Holland and Redfern 1997). In addition, zero shift and silicon lattice parameters were derived using the same experimental and analytical procedures on a NBS silicon standard. Run products were further characterized using a JEOL scanning electron microscope (GRC) equipped with an EDX spectrometer (EDXS). For quantitative analysis, the microscope is operated at 15 kV (0.885 nA), a ZAF correction is applied and a cobalt reference standard is used for instrumental calibration. The most interesting specimens were further analyzed using a SX100 electron microprobe (10 nA, 15 kV) using fluorapatite (P), albite (Na), orthoclase (Al), and diopside (Mg, Si) as standards.

Table 1. Starting-material composition

Composition	Starting-material preparation
Si_0P_3	Na_2CO_3, $NH_4H_2PO_4$, Al_2O_3*
$Si_{0.25}P_{2.75}$	MgO, Al_2O_3 gel, SiO_2, Na_2CO_3, $NH_4H_2PO_4$
Si_1P_2	SiO_2, $MgAl_2O_4$, Na_2CO_3, $NH_4H_2PO_4$
$Si_{1.25}P_{1.75}$	MgO, SiO_2, $MgAl_2O_4$, Na_2CO_3, $NH_4H_2PO_4$
$Si_{1.5}P_{1.5}$-g	TEOS-based gel with $NH_4H_2PO_4$, $Mg(NO_3)_3$, Na_2CO_3, and $Al(NO_3)_3$†
$Si_{1.75}P_{1.25}$	MgO, SiO_2, $MgAl_2O_4$, Na_2CO_3, $NH_4H_2PO_4$
Si_2P_1	MgO, SiO_2, $MgAl_2O_4$, Na_2CO_3, $NH_4H_2PO_4$
Si_2P_1-g	TEOS-based gel with $NH_4H_2PO_4$, $Mg(NO_3)_3$, Na_2CO_3, and $Al(NO_3)_3$†
$Si_{2.5}P_{0.5}$	MgO, Al_2O_3 gel, SiO_2, Na_2CO_3, $NH_4H_2PO_4$

Note: Each starting material has been baked over 600 °C before use.
* See Brunet et al. (2003).
† See Brunet and Chazot (2001).

Table 2. Experimental results

Composition	*T* (°C)	*P* (GPa)	Duration (h)	Phase identification (XRD and SEM)	Unit-cell volume (Å^3)
Si_0P_3	1600	17	14	garnet + cor. *	1553.3(9)
Si_0P_3	1400	17	6	garnet + (?)	1552.5(6)
$Si_{0.25}P_{2.75}$	1400	17	7.3	garnet + stish. + cor.	1555.8(1.2)
Si_1P_2	1400	17	6.5	garnet + cor. + stish.	1545.8(7)
Si_1P_2	875	3	139	?? + jad. + cor. + berl.	–
$Si_{1.25}P_{1.75}$	1400	17	7.3	garnet + stish. + cor. + (α-$NaMgPO_4$)	1542.8(5)
$Si_{1.5}P_{1.5}$-g	1400	17	6	stish. + α-$NaMgPO_4$ + garnet	–
$Si_{1.75}P_{1.25}$	1600	17	14	garnet + cor. + stish. + α-$NaMgPO_4$+ (???)*	1519.1(1.1)
Si_2P_1	1400	15	6	garnet + cor. + stish. + α-$NaMgPO_4$	1535(4)
Si_2P_1	875	3	139	garnet + ?? + jad. + ber. + cor.	1506.6(6)
Si_2P_1-g	1250	17	9	stish. + garnet + α-$NaMgPO_4$	1516.3(1.1)
$Si_{2.5}P_{0.5}$	1400	15	6	garnet + stish. + cor. + α-$NaMgPO_4$	1516.3(2.1)
$Si_{2.5}P_{0.5}$	875	3	139	garnet + jad. + cor. + ?? + ber	1504.2(5)

Notes: cor = corundum, stish = stishovite, jad = jadeite, ber = berlinite, $AlPO_4$. Phases in parentheses are present in trace amounts whereas bold phases are dominant phases on the XRD pattern. ? = extra phase identified from Rietveld refinement (see text). ?? = unidentified phase likely to be an Mg-phosphate of alluaudite structure (main diffraction lines, 2θ Cu$K\alpha$ at 33.7 and 33.0). ??? = third unidentified phase (main diff. lines, 2θ: 24.2 and 34.2). Unit-cell volumes are given to (±3σ), NBS silicon-standard yields a = 5.4302 Å (σ = 0.0001 Å).
* Evidence for partial melting (see text).

Results

Eight different compositions have been investigated along the $Mg_3Al_2(SiO_4)_3$-$Na_3Al_2(PO_4)_3$ join. They will be named hereafter according to their Si:P content pfu (i.e., on a 12 oxygen basis), Si_0P_3, $Si_{0.25}P_{2.75}$, Si_1P_2, $Si_{1.25}P_{1.75}$, $Si_{1.5}P_{1.5}$, $Si_{1.75}P_{1.25}$, Si_2P_1, and $Si_{2.5}P_{0.5}$, respectively (Table 1). Experimental results, including phase identification by XRD and SEM, are summarized in Table 2. Apart from the Si_1P_2 nominal composition held at 3 GPa and 875 °C, all run products display an XRD pattern showing the presence of a garnet-structure compound (Fig. 1). This holds also true for the $Na_3Al_2(PO_4)_3$ composition (Fig. 1) indicating that a garnet-type phosphate end-member has been obtained. Garnet structure (I*a-3d*) was confirmed by Rietveld refinement (GSAS package, Larson and Von Dreele 2000). Unit cell, profile function, and background parameters were first derived using Lebail whole-pattern fitting assuming I*a-3d* as space group. The refined XRPD pattern (Fig. 1) shows the presence of a few unindexed diffraction peaks significantly broader than the garnet ones, which are therefore interpreted as belonging to unidentified extra phase(s). Convergence was achieved (R_p = 12%, χ^2 = 3.6) using pyrope atomic coordinates (Novak and Gibbs 1971) and refining the oxygen position only [x = 0.046(1), y = 0.045(1), z = 0.658(1)]. This refined oxygen position, in the phosphate garnet, leads to acceptable average cation-oxygen distances of 1.50 Å, 1.97 Å, and 2.39 Å for tetrahedral (P), octahedral (Al), and dodecahedral (Na) sites, respectively. Although the garnet structure is confirmed, the quality of the diffraction pattern, collected on 2–3 mg of powder only, and the presence of unidentified products (with peak overlap with $Na_3Al_2(PO_4)_3$ – garnet, Fig. 1) prevented more reliable refinement of oxygen coordinates and refinement of the isotropic displacement factors. Characteristic garnet diffraction peaks in the high-pressure experiments (15–17 GPa range) are shifted toward smaller diffraction angles from silicon- to phosphorus-rich compositions, indicative of an increase of the garnet unit-cell dimension (Fig. 1, Table 2). Stishovite, corundum, and possibly α-$NaMgPO_4$ (JCPDS 32-1119) occur as by-products of the garnet synthesis (Table 2). Although anhydrous, garnet syntheses yielded grains of several micrometers across (Fig. 2). Partial melting has occurred in two samples run at 1600 °C (Si_0P_3 and $Si_{1.75}P_{1.25}$) as indicated by textural observation and confirmed by the strong sintering noticed when grinding the sample for XRD. In both cases, however, the corresponding diffraction pattern yields garnet as the dominant phase. Furthermore, for the

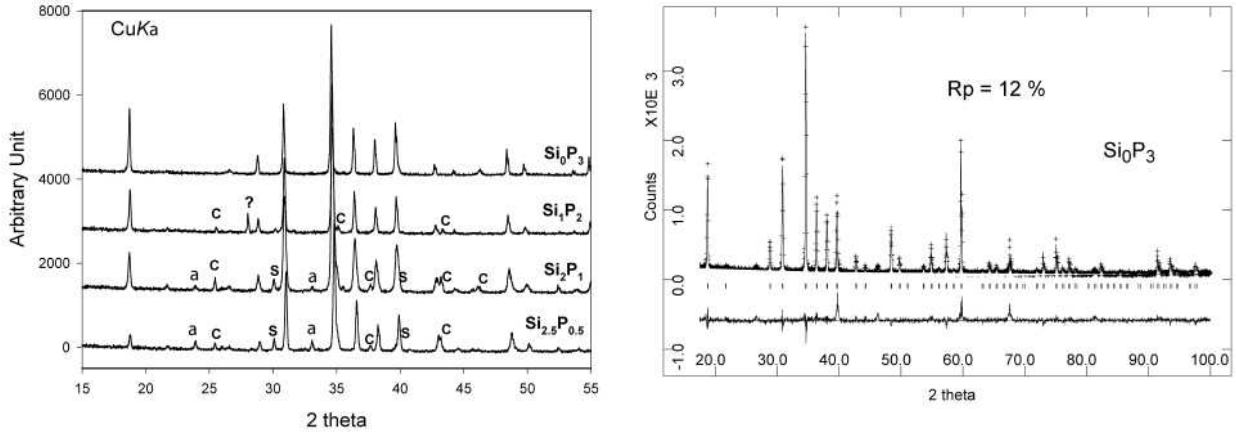

FIGURE 1. X-ray powder diffraction patterns of the experimental products: Si_0P_3 (1400 °C, 17 GPa, 6 hours), S_1P_2 (1400 °C, 17 GPa, 6.5 hours), Si_2P_1 (1400 °C, 15 GPa, 6 hours), and $Si_{2.5}P_{0.5}$ (1400 °C, 15 GPa, 6 hours). The diffraction peaks of the main extra phases are marked, "**C**" for corundum,"**S**" for stishovite, and "α" for α-$NaMgPO_4$. *On the right*: graphical output of the Si_0P_3 Rietveld refinement (1400 °C, 17 GPa, 6 hours) in the garnet structure (I*a*-3*d*). Observed pattern is outlined by crosses. Note the presence, in the refinement residue, of extra reflections at 2θ = 26.6, 33.0, *39.7*, *46.3*, 59.7, *67.6,* and *81.3*° (values in italics may correspond to platinum reflections).

Si_0P_3 composition held at 1400 °C and 17 GPa, phosphate-garnet crystals are euhedral (Fig. 2) and cannot be related to quench. Electron microprobe analyses of the garnet phases are plotted in a compositional triangle (Si-Al-P, Fig. 3a). As much as possible, electron microprobe data have been acquired on homogeneous crystals as inferred from secondary electron imaging, with sizes above a few micrometers. Among these microprobe data, we only considered in Figure 3 those with totals between 95 and 102

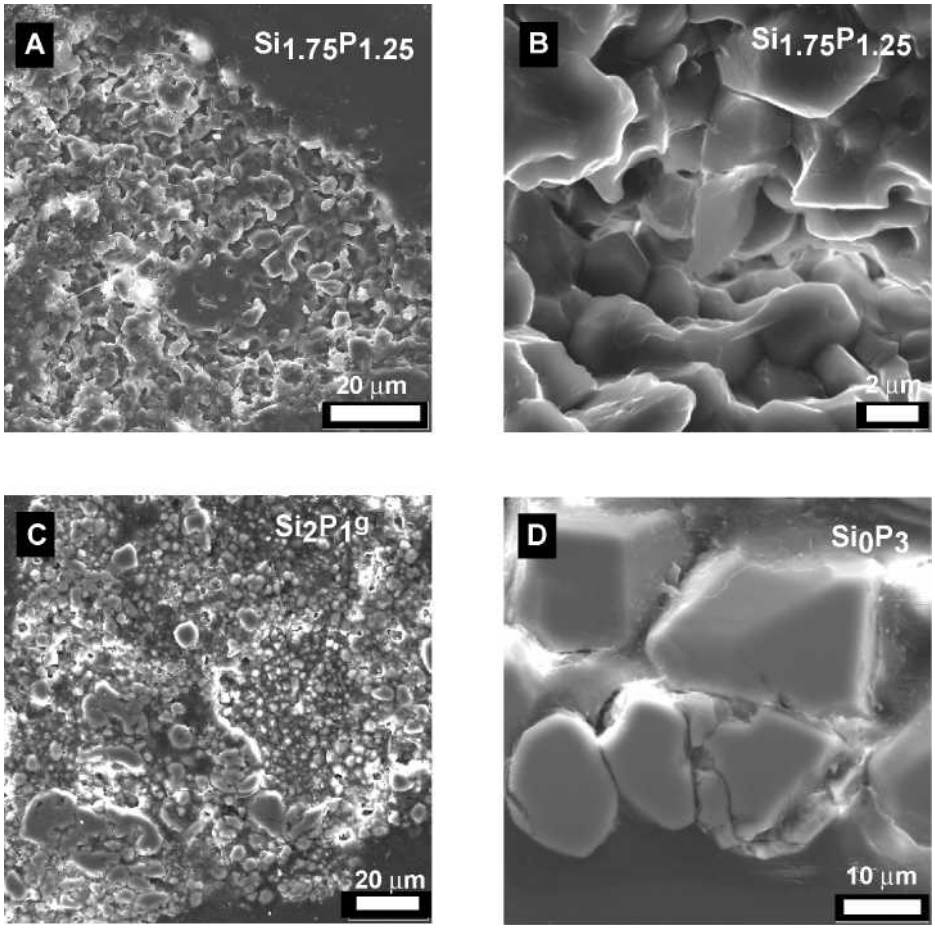

FIGURE 2. SEM images of garnet grains in secondary electron mode. (**a** and **b**) $S_{1.75}P_{1.25}$ (1600 °C, 17 GPa, 14 hours), (**c**) Si_2P_1-g (1250 °C, 17 GPa, 6 hours), (**d**) Si_0P_3 (1400 °C, 17 GPa, 6 hours).

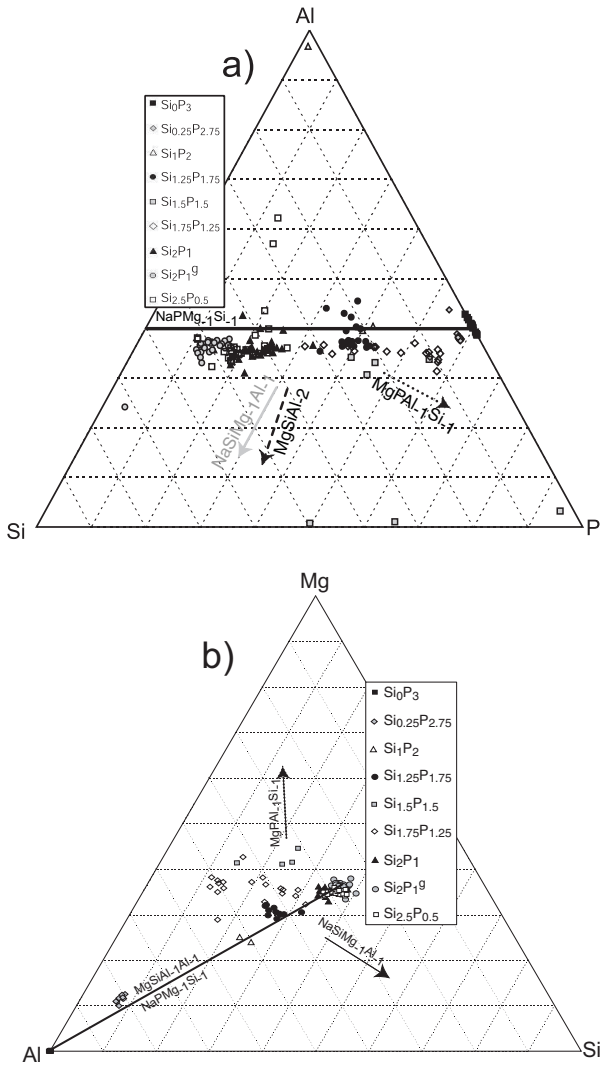

FIGURE 3. Selected EMP garnet analyses plotted in an Al-Si-P (**a**) and an Al-Si-Mg (**b**) compositional triangle. Substitution vectors are indicated with arrows.

wt%. Furthermore, structural formulae have been recalculated, and data with cation sums lying out of the 7.8 and 8.1 pfu range have also been rejected.

Compared to their nominal compositions, garnets are slightly depleted in Al relative to Si + P. This relative depletion is marked toward high phosphorus contents up to the $Si_{1.25}P_{1.75}$-Si_1P_2 compositions whereas both Si_0P_3 and $Si_{0.25}P_{2.75}$ compositions plot close to the $NaPMg_{-1}Si_{-1}$ tie-line (Fig. 3a). In an Al-Si-Mg triangle (Fig. 3b), silicon-rich garnets plot on the expected $MgSiAl_{-1}Al_{-1}$ line (superposed to the $MgSiNa_{-1}P_{-1}$ line in this diagram). When the P-content increases, the garnet compositions lie out of that latter line on the Mg-rich side of the triangle. This indicates that an $MgPAl_{-1}Si_{-1}$ substitution vector is partly responsible for the Al-deficiency in these garnets.

The volume of the garnet unit cell is plotted as a function of nominal composition (or bulk composition measured in scanning mode for products derived from gels) in Figure 4. For the end-member composition, $Mg_3Al_2(SiO_4)_3$, the pyrope volume by Hazen and Finger (1978) is displayed and that of $MgSiO_3$ majorite (Angel et al. 1989) is also plotted to reveal the effect of majoritic component on unit-cell volume. The unit-cell volume of synthetic garnet increases by 3.1% from the phosphorus-free to the silicate-free composition. The Si_0P_3 volume (obtained on two different samples) plots far below the extrapolation of the volume-Si-content function derived from Si_3P_0 up to Si_1P_2 (Fig. 4). The unit-cell volumes of the garnets obtained at 3 GPa on the $Si_{2.5}P_{0.5}$ and Si_2P_1 nominal compositions are close to end-member pyrope volume. Therefore, compared to the counterpart syntheses obtained at 15 GPa, these lower pressure garnets incorporated much less phosphorus.

DISCUSSION

Brunet et al. (2003) derived experimentally the $Na_3Al_2(PO_4)_3$ phase diagram up to 8 GPa. By analogy to the polymorphism of $Na_3Fe_2(AsO_4)_3$ and $Na_3Cr_2(AsO_4)_3$, they proposed that a $Na_3Al_2(PO_4)_3$ garnet-modification could take place at high-pressure (i.e., above 8 GPa) and that this modification should exhibit an *a*-parameter comprised between 11.5 and 11.6 Å at ambient conditions. This assumption is confirmed by the present study, where, for the first time, a phosphate garnet of $Na_3Al_2(PO_4)_3$ composition is obtained and characterized. The measured cubic unit-cell parameter of 11.579(2) Å agrees well with the expected value. In a brief communication, Thilo (1941) claimed to have synthesized a similar garnet from cooling a molten Na_3PO_4 + $AlPO_4$ mixture at ambient pressure. However, as discussed in Brunet et al. (2003) and as confirmed here, the synthesis of a $Na_3Al_2(PO_4)_3$ garnet at ambient pressure is unlikely.

In the experimental conditions investigated here (*P*, *T*, and composition), a complete solid-solution between pyrope and $Na_3Al_2(PO_4)_3$ is found although $Na_3Al_2(PO_4)_3$ is only a very minor

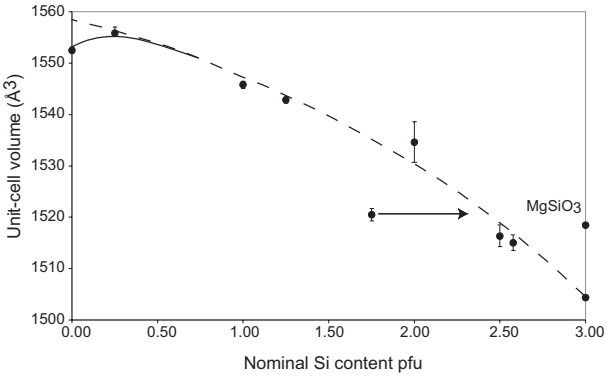

FIGURE 4. Volume of the garnet unit cell as a function of Si-content pfu. This Si-content is recalculated from the nominal Si-content of the starting material for products obtained from oxide mixtures whereas it corresponds to the Si-content measured by SEM (on a 5.10^{-2} mm^2 area) for products obtained from gels. Unit-cell volumes of pyrope, $Mg_3Al_2(SiO_4)_3$, and $MgSiO_3$ garnet are from Hazen and Finger (1978), and Angel et al. (1989), respectively. The point that plots far from the trend (dashed line) corresponds to the $Si_{1.75}P_{1.25}$-g suspected to have encountered partial melting (see text).

component in natural garnets. Actually, the $MgSiNa_{-1}P_{-1}$ substitution alone cannot account for the synthetic garnet compositions and especially for the Al deficiency. Aluminum deficiency in high-pressure garnets is often attributed to a majorite component. It appears, however, that the $MgPAl_{-1}Si_{-1}$ substitution accounts for part of the Si-P replacement as illustrated by tb where several data points plot above the majoritic join on the Mg side of the triangle. The occurrence of two independent substitutions may partly explain the scattering of the unit-cell volume – composition data (Fig. 4). For example, as far as the end-member phosphate garnet is concerned, the octahedral site is fully occupied by Al (e.g., neither octahedral P nor Na). Its composition is therefore fully accounted for by a single substitution vector, $NaPMg_{-1}Si_{-1}$. This may explain why its volume departs from the trend followed by the other garnets, the composition of which results from at least two substitution types. The $AlSiMg_{-1}P_{-1}$ one involves a tetrahedral silicon-phosphorus replacement coupled with the substitution of magnesium for octahedral aluminum. It has already been reported in the UHP ellenbergerite solid-solution series (Chopin and Sobolev 1995). In contrast to garnets, pressure stabilizes the silicate ellenbergerite end-member (Brunet et al. 1998). In both cases, however, molar volume increases toward the phosphate end-member (by ca. 4.3% along the ellenbergerite series).

The likely stability of $Na_3Al_2(PO_4)_3$ garnet (only synthesis experiments have been carried out here) under deep Earth conditions has two important consequences.

First, the potential of silicates to host phosphorus in the upper mantle (Thompson 1975; Brunet and Chazot 2001) is confirmed and garnet appears as a good candidate as a P-repository in the mantle (Haggerty et al. 1994) where primary phosphate minerals might not be expressed at all. Second, the P-content of UHP garnet from the Dora-Maira massif can be seen as a consequence of high pressures. Phosphate minerals, which coexist with garnet in the UHP paragenesis (e.g., Chopin et al. 1993; Brunet et al. 1998) are likely to buffer the phosphorus content in garnet.

Therefore, the P (and Na) content of Dora-Maira pyropes is a potential pressure indicator like the P content in the ellenbergerite series (Chopin and Sobolev 1995; Brunet et al. 1998). In the case of upper-mantle garnets, which barely coexist with phosphate minerals, the P-content rather reflects phosphorus availability. In this case, phosphorus content in garnet is a measure of phosphorus activity in the garnet host-rock. Since phosphorus diffusion kinetics in garnet is low, phosphorus distribution in garnet can help to decipher growth history, for example through preserved growth zones (e.g., Vielzeuf et al. 2005).

ACKNOWLEDGMENTS

Frederic Hatert and an anonymous referee are greatly acknowledged for their constructive reviews. Daizuke Yamazaki is thanked for sharing his unlimited knowledge of the multi-anvil science, Frédéric Couffignal for running the microprobe at Camparis (Paris VI). FB stay at GRC was financially supported by a JSPS fellowship and by the CNRS.

REFERENCES CITED

Angel, R.J., Finger, L.W., Hazen, R.M., Kanzaki, M., Weidner, D.J., Liebermann, R.C., and Veblen, D.R. (1989) Structure and twinning of single-crystal $MgSiO_3$ garnet synthesized at 17 GPa and 1800 °C. American Mineralogist, 74, 509–512.

Bishop, F.C., Smith, J.V., and Dawson, J.B. (1978) Na, K, P and Ti in garnet, pyroxene and olivine from peridotite and eclogite xenoliths from African kimberlites. Lithos, 11, 155–173.

Brunet, F. and Chazot, G. (2001) Partitioning of phosphorus between olivine, clinopyroxene and silicate glass in a spinel lherzolith from Yemen. Chemical Geology, 176, 51–72.

Brunet, F. and Lecocq, D. (1999) Phosphorus incorporation in garnet: natural and experimental data. European Journal of Mineralogy, 11, 43.

Brunet, F., Chopin, C., and Seifert, F. (1998) Phase relations in the MgO-P_2O_5-H_2O system and the stability of phosphoellenebergerite: petrological implications. Contribution to Mineralagy and Petrology, 131, 54–70.

Brunet, F., Bagdassarov, N., and Miletich, R. (2003) $Na_3Al_2(PO_4)_3$, a fast sodium conductor at high pressure: in-situ impedance spectroscopy characterisation and phase diagram up to 8 GPa. Solid State Ionics, 159, 35–47.

Chopin, C. and Sobolev, N. (1995) Principal mineralogical indicators of UHP in crustal rocks. In R.G. Coleman and X. Wang, Eds., Ultra-high pressure metamorphism, p. 97–131. Cambridge University Press, U.K.

Chopin, C., Brunet, F., Gebert, W., Medenbach, O., and Tillmans, E. (1993) Bearthite, $Ca_2Al(PO_4)_2OH$, a new mineral from high-pressure terranes of the western Alps. Schweizerische Mineralogische und Petrographische Mitteilungen, 73, 1–9.

Compagnoni, R. and Hirajima, T. (2001) Superzoned garnets in the coesite-bearing Brossasco-Isasca Unit, Dora-Maira Massif, Western Alps, and the origin of the whiteschists. Lithos, 57, 219–236.

Haggerty, S.E., Fung, A.T., and Burt, D.M. (1994) Apatite, phosphorus and titanium in eclogitic garnet from upper mantle. Geophysical Research Letters, 21, 1699–1702.

Hazen, R.M. and Finger, L.W. (1978) Crystal structures and compressibilities of pyrope and grossular to 60 kbar. American Mineralogist, 63, 297–303.

Holland, T.J.B. and Redfern, S.A.T. (1997) Unit cell refinement from powder diffraction data: the use of regression diagnostics. Mineralogical Magazine, 61, 65–77.

Larson, A.C. and Von Dreele, R.B. (2000) General structure analysis software (GSAS). Los Alamos National Laboratory, Report LAUR 86–748.

McCandless, T.E. and Gurney, J.J. (1989) Sodium in garnet and potassium in clinopyroxene; criteria for classifying. In J. Ross, A.L. Jaques, J. Ferguson, D.H. Green, S.Y. O'Reilly, R.V. Danchin, and A.J.A. Janse, Eds., Kimberlites and related rocks. Proceedings of the fourth international kimberlite conference. Geological Society of Australia, Sydney, N.S.W., Australia, p. 827–832.

Meagher, E.P. (1980) Silicate garnets. In P.H. Ribbe, Ed., Orthosilicates, 5, p. 25–66. Reviews in Mineralogy, Mineralogical Society of America, Chantilly, Virginia.

Moore, R.O. and Gurney, J.J. (1985) Pyroxene solid solution in garnets included in diamond. Nature, 318, 553–555.

Novak, G.A. and Gibbs, G.V. (1971) The crystal chemistry of the silicate garnets. American Mineralogist, 56, 791–825.

Reid, A.M., Brown, R.W., Dawson, J.B., Whitfield, G.G., and Seibert, J.C. (1976) Garnet and pyroxene compositions in some diamondiferous eclogites. Contribution to Mineralogy and Petrology, 58, 203–220.

Ringwood, A.E. and Major, A. (1971) Synthesis of majorite and other high-pressure garnets and perovskites. Earth and Planetary Science Letters, 12, 411–441.

Schulze, D.J. (1992) Diamond eclogite from Sloan Ranch, Colorado, and its bearing on the diamond grade of the Sloan kimberlite, Economic Geology, 87, 2175–2179.

Shertl, H.-P., Schreyer, W., and Chopin, C. (1991) The pyrope-coesite rocks and their country rocks at Parigi, Dora Maira Massif, Western Alps: detailed petrography, mineral chemistry and PT-path. Contribution to Mineralogy and Petrology, 108, 1–21.

Smith, J.V. and Mason, B. (1970) Pyroxene-garnet transformation in Coorara Meteorite. Science, 168, 832–833.

Sobolev, N.V. and Lavrent'ev, J.G. (1971) Isomorphic sodium admixture in garnets formed at high pressures. Contribution to Mineralogy and Petrology, 31, 1–12.

Sobolev, N.V. and Shatsky, V.S. (1990) Diamond inclusions in garnets from metamorphic rocks: a new environement for diamond formation. Nature, 343, 642–745.

Thilo, E. (1941) Über die Isotypie zwischen Phosphaten der allgemeinen Zusammensetzung $(Me^1)_3(Me^2)_2[PO_4]_3$ und den Silikaten der Granatgruppe. Naturwissenschaften, 29, 239.

Thompson, R.N. (1975) Is upper mantle phosphorus contained in sodic garnet? Earth and Planetary Science Letters, 26, 417–424.

Vielzeuf, D., Veschambre, M., and Brunet, F. (2005) Oxygen isotope heterogeneities and diffusion profile in composite metamorphic-magmatic garnets from Pyrenees. American Mineralogist, 90, 463–472.

Ye, K., Cong, B., and Ye, D. (2000) The possible subduction of continental material to depths greater than 200 km. Nature, 407, 734–736.

MANUSCRIPT RECEIVED AUGUST 2, 2005
MANUSCRIPT ACCEPTED SEPTEMBER 14, 2005
MANUSCRIPT HANDLED BY BRYAN CHAKOUMAKOS